Terrain-Dependent Motion Adaptation for Hexapod Robots

Timon Homberger[1,2], Marko Bjelonic[1,3],
Navinda Kottege[1], and Paulo V. K. Borges[1]

[1] Autonomous Systems Lab, CSIRO, Brisbane, QLD 4069, Australia
[2] Department of Mechanical and Process Engineering, ETH Zurich, 8092 Zurich, Switzerland
[3] Faculty of Mechanical Engineering, Technische Universität Darmstadt, 64287 Darmstadt, Germany.

1 Introduction

Locomotion of mobile robots on rough terrain, without prior information on terrain structure is an important task. It is required for planetary exploration [1], missions in disaster zones [2], mining [3], and others. In this field, legged robots have gained increased attention [4], due to their mechanical ability to move on various types of challenging terrain.

The efficiency of terrain traversal highly depends on the robots gait structure, i.e. on the parameters of the leg motion. Aiming for smooth and efficient maneuvering on variably cluttered ground, we present a new design of a robot-terrain interaction system, which combines proprioceptive and exteroceptive terrain adaptation. A highly flexible hexapod robot (30 degrees of freedom), is equipped with a vision based motion adaptation system. The latter uses amongst others a novel method for feature extraction, the 'even run length' as well as terrain feature evaluation methods for accurate characterization of a large number of terrain types. (section 2)

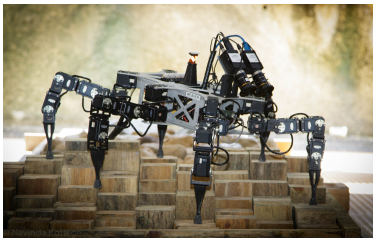

Fig. 1. Hexapod robot 'Weaver' with Stereo Camera System

The hexapod platform features 5 joints per leg, allowing motion stability on unstructured terrain, i.e. the robot is able to align the foot tips with the gravity vector, independent of the pose of the robots body. [5]. The legs are controlled in analogy to a mass-spring-damper system. This impedance control lets the robot

handle unforeseen changes in local elevation by maintaining contact between the foottips and the ground at almost any time. [5].

Low virtual stiffness values for the robot legs allows traversing very uneven and cluttered terrain, while the robot would get stuck (velocity approaching zero) if the legs are very stiff. In mathematical terms, the CoT tends to infinity when the velocity approaches zero. It was also found that with low stiffness values, CoT is high for motion on flat, hard terrain. [5] Therefore, a way to minimize the cost is to adapt the stiffness to the terrain structure, which the robot is moving on. Similarly the height of the robots stride is to be adapted. The combined application of adaptive stride height and adaptive impedance is expected to substantially reduce transport cost compared to non adaptive locomotion on rough terrain. A calibrated stereo camera system is used to generate 3D information of the terrain, which forms the robots path ahead. This information is used to extract various ground features, which are mathematically combined to generate priors to the leg joint stiffness and the stride height, thus allowing the system to enhance efficiency of rough terrain traversal.

2 Technical Approach

By generating a disparity map (fig. 3), depth information of the scene, which is perceived by the cameras, is gained and stored as a point cloud of points in 3D space. This point cloud is downscaled using a voxel grid filter [6] and by using Inertial Measurement Unit (IMU) data, it is transformed into a coordinate system, which is aligned with the gravity vector. This allows terrain intrinsic feature extraction [**?**] [6]. A Digital Elevation Model (DEM), [7] [8] is generated by discretizing the horizontal plane into quadratic cells. A DEM point cloud is generated, marking the maximum terrain elevation of each cell with a DEM point. (fig. 3)

After fitting a plane into the data, (Least Squares method) a set of terrain features, particularly designed for rough terrain characterization, is extracted from an approximately robot sized surface area.(fig. 2)

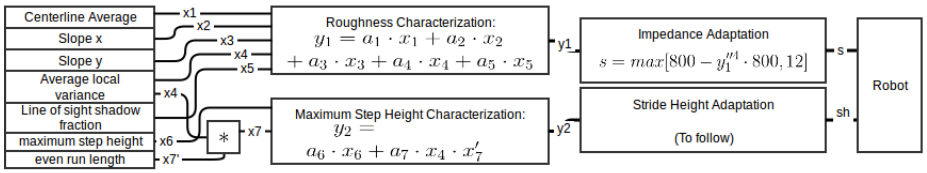

Fig. 2. Overview on terrain adaptive motion control. Extracted features: centerline average x_1 [**?**], slope x_2 and x_3 (slope of the fitted plane in longitudinal and lateral direction respectively), average local variance x_4, shadows caused by line of sight limitations x_5 [9], maximum step height x_6 and run length quantification x_7.

'Even Run Length' is a novel method to quantify the amount of continuous, nearly-horizontal surfaces. It is adapted from grey scale image analysis meth-

ods [10]. The shadows caused by line of sight limitations take into account the fraction of the surface, which due to geometrical reasons can not be observed by the cameras [9]. The system classifies unobservable sections as uncertainties and thus chooses motion parameters more conservatively. Local variance and maximum step height are calculated by a 'local descriptor' method, similarly used in [6] and [8].

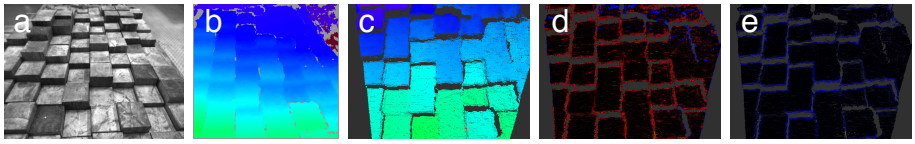

Fig. 3. Left camera image (a), corresponding disparity map (b), DEM Point Clouds in three different color schemes: Terrain elevation (c), local variance (d) with red → high value and step height (e) with blue → high value.

From these extracted features x_i two descriptive ground characterization parameters, roughness y_1 and maximum step height y_2, are derived. They serve for impedance and stride height adaptation respectively.(fig. 2) Note, that the formula for Step Height Characterization includes the term: $a_7 \cdot x_4 \cdot x'_7$. This value quantifies the occurrence of nearly planar surfaces which are bordered by extremely steep slopes. Areas, which contain a lot of such planar surfaces require high stride height to be smoothly traversed.

3 Experiments

For comparative evaluation of performance, a multi-terrain testbed of 7.9 m length was used. It consists of patches of 6 different terrain types (fig. 4). The experiments consisted of the hexapod robot repeatedly traversing on this testbed[4] with high level navigation (velocity commands) provided by a human operator via a controller.

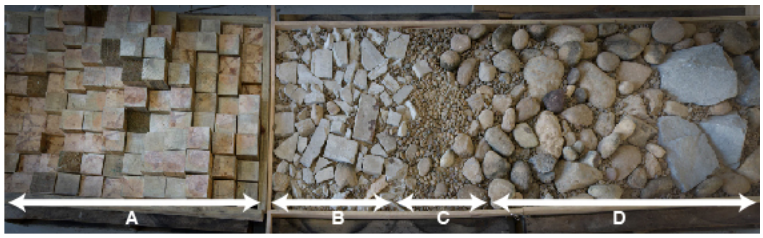

Fig. 4. Sections A to D of the Testbed. 2.93 m of flat ground (Section 0) followed by 1.2 m of inclined planar section (10°) (Section 1) are traversed before entering Section A.

[4]Video available here: https://wiki.csiro.au/display/ASL/ISER2016Stereo

As the robot perceives terrain features at a given distance upfront of the platform, information on ego-motion is needed. For future outdoor application, localization is to be achieved using visual odometry or visual-inertial odometry. This is motivated by the fact, that the robot contains the required hardware for this task (IMU data is available. [5]) To track the robot pose and thus simulate visual odometry, a robotic total station (Leica TS12) was used during testing. The total station tracks a reflector prism attached to the robot and provides its 3D position. For evaluation of the motion efficiency, the cost of transport (CoT) defined as $CoT = P/mgv$ [11] is calculated. P is the power consumption, mg is the mass of the robot and v is the velocity. P is calculated by monitoring the voltage and current draw during the experiments.

3.1 Conducted Experiments

Two sets of 5 runs each have been conducted to examine the cost of transport. Adaptive impedance control was used during the first set and constant stiffness was applied in the second set. For adaptive impedance control, a set of valid weighting parameters a_i were found by conducting tests in critical sections ensuring traversability on the testbed (fig. 2, fig. 4).

The constant stiffness is the minimum of the range of stiffness values of the adaptive impedance control (i.e. $12\,\mathrm{Nm}^{-1}$). (see eq. (1)) It is chosen such, that it suffices to overcome the most difficult sections of the test track (A and D). [see fig. 4]

4 Results

A correlation of stiffness s and roughness characterization y_1, that leads to good performance of adaptive impedance control on the testbed, was empirically derived.

$$s = max[800 - y_1^4 \cdot 800, 12] \tag{1}$$

eq. (1) was found to yield sufficiently low stiffness ($12\,\mathrm{Nm}^{-1}$) for high values of y_1 but very high stiffness values for small y_1. The latter benefits efficient motion on rather flat terrain (see fig. 5). Stride height adaption is to be achieved similarly. Details on scheduled experiments can be found in section 5.

fig. 5 shows the resulting CoT of the experiments described in section 3.1. The difference in CoT in sections 0 and 1, can be explained by angular and vertical robot body motion, which occurs if walking on flat ground with a low stiffness. The CoT reduction of adaptive impedance control is especially high in section 1, as the body motion (non-adaptive case) causes instability and slippage on the slope. Section A shows no difference of CoT. This is as expected since the same stiffness is applied in both cases. In section B, the adaptive approach has clear advantages compared to the non-adaptive case. High CoT values in the

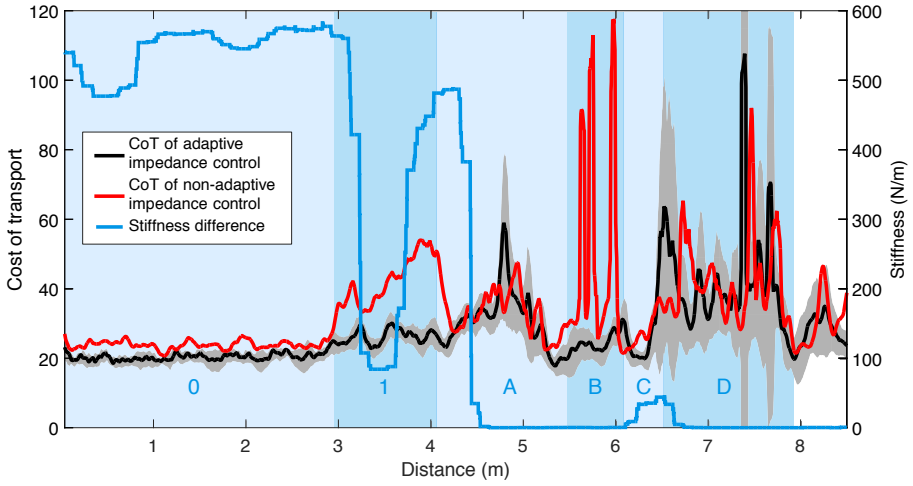

Fig. 5. CoT for adaptive and non-adaptive impedance control, results of 5 runs on the test track each. (See fig. 4)

non-adaptive case imply that the robot has difficulties to traverse the terrain. In the last two sections equal stiffness parameters lead to similar CoT in both cases.

5 Experimental Insights

The experiment described in section 4 shows, that CoT can be reduced significantly by applying adaptive impedance control. The robot manages to safely traverse the testbed and shows similar performance on very uneven terrain for both control types (I.e. the most challenging sections A and D).

Realization of stride height control is similar as is the realization of adaptive impedance control. It aims for reduced CoT on rather flat terrain, but to allow maneuvering on difficult terrain or steep slopes. The height of the hexapods stride is to be set as a function of the step height quantification parameter y_2 (fig. 2) and similar tests are to be conducted as described in section 3.1.

The combined application of adaptive impedance and stride height control may lead to further reduction of the CoT. It can be problematic to find adequate weighting parameters for the roughness and the step height quantification respectively (fig. 2), as this entire set of parameters influences robot maneuverability. E.g. maneuvering in an area with given terrain structure, the choice of stride height limits the range of leg joint stiffness values which lead to successful traversal. Analysing interdependency of y_1 and y_2 (s and sh respectively) and setting constraints on their ranges is the goal of the conducted experiments. Thereby the ability of the combined application of adaptive impedance control and adaptive stride height control to further increase locomotion efficiency is

to be proven. Training based optimization methods (e.g. Levenberg-Marquardt) are considered to be applied in order to minimize power consumption.

As a special case, motion on soft terrain is to be examined (e.g. on grassland or sand). In this case, there is a discrepancy between visual perception of terrain and proprioceptive perception of terrain. The latter is obtained by calculating the foot tip positions of the robot, using forward kinematics. [5] Thus, by quantifying the discrepancy between exteroceptive and proprioceptive terrain perception, a ground softness characterization can be derived. This fusion of information sources allows enhanced locomotion efficiency on soft ground.

These experiments reveal insights on the potential of adaptive motion control on uneven terrain in terms of traversability and transport cost minimization. This covers the extractability and fusion of terrain information, the (combined) usage of stride-height control and impedance control, as well as a novel approach to ground softness characterization, which is obtained by comparing exteroceptive and proprioceptive terrain perception. Experiments are conducted on the test track(fig. 4), similarly as described in section 3, as well as on an extensive set of outdoor terrains, featuring varying slope, softness, unevenness and lighting conditions, in order to validate the innovative approaches to robot-terrain interaction.

References

1. Howard, A.: Real-time stereo visual odometry for autonomous ground vehicles. In: IEEE/RSJ International Conference on Intelligent Robots and Systems (IROS). (2008) 3946–3952
2. Ohki, T., Nagatani, K., Yoshida, K.: Path planning for mobile robot on rough terrain based on sparse transition cost propagation in extended elevation maps. In: IEEE International Conference on Mechatronics and Automation (ICMA). (2013) 494–499
3. Li, G., Song, R., Chen, C., Li, Y., Zhang, C.: The traversability analysis for coal mine mobile robot based on rough sets. In: IEEE International Conference on Robotics and Biomimetics (ROBIO). (2013) 420–424
4. Hauser, K., Bretl, T., Latombe, J.C., Harada, K., Wilcox, B.: Motion planning for legged robots on varied terrain. The International Journal of Robotics Research **27**(11-12) (2008) 1325–1349
5. Bjelonic, M., Kottege, N., Beckerle, P.: Proprioceptive control of an over-actuated hexapod robot in unstructured terrain. In: IEEE/RSJ International Conference on Intelligent Robots and Systems (IROS). (2016) 2042–2049
6. Bellone, M., Reina, G., Giannoccaro, N.I., Spedicato, L.: Unevenness point descriptor for terrain analysis in mobile robot applications. International Journal of Advanced Robotic Systems **10** (2013)
7. Aeschimann, R., Borges, P.V.K.: Ground or obstacles? detecting clear paths in vehicle navigation. In: IEEE International Conference on Robotics and Automation (ICRA). (2015) 3927–3934
8. Chilian, A., Hirschmüller, H.: Stereo camera based navigation of mobile robots on rough terrain. In: IEEE/RSJ International Conference on Intelligent Robots and Systems (IROS). (2009) 4571–4576

9. Kolter, J.Z., Kim, Y., Ng, A.Y.: Stereo vision and terrain modeling for quadruped robots. In: IEEE International Conference on Robotics and Automation (ICRA). (2009) 1557–1564
10. Theodoridis, S., Koutroumbas, K.: Pattern Recognition, Third Edition. Academic Press, Inc., Orlando, FL, USA (2006)
11. Kottege, N., Parkinson, C., Moghadam, P., Elfes, A., Singh, S.P.N.: Energetics-informed hexapod gait transitions across terrains. In: IEEE International Conference on Robotics and Automation (ICRA), IEEE (2015) 5140–5147